


Article

# Synthesis and Characterization of Aluminum 2-Carboxyethyl-Phenyl-Phosphinate and Its Flame-Retardant Application in Polyester

Zhongying Yao <sup>1,2</sup>, Xinxin Liu <sup>3,†</sup>, Lijun Qian <sup>1,2,\*</sup> , Yajun Chen <sup>1,2</sup>, Bo Xu <sup>1,2</sup> and Yong Qiu <sup>1,2</sup>

<sup>1</sup> School of Materials Science and Mechanical Engineering, Beijing Technology and Business University, Beijing 100048, China; yzybtbu@163.com (Z.Y.); chenyajun@th.btbu.edu.cn (Y.C.); xubo@btbu.edu.cn (B.X.); yongqiu@btbu.edu.cn (Y.Q.)

<sup>2</sup> Engineering Laboratory of Non-Halogen Flame Retardants for Polymers, Beijing 100048, China

<sup>3</sup> National-Certified Enterprise Technology Center, Kingfa Science and Technology Co., Ltd., Guangzhou 510520, China; lxxbtbu@163.com

\* Correspondence: qianlj@th.btbu.edu.cn; Tel.: +86-10-68984011

† The joint first author.

Received: 10 October 2019; Accepted: 20 November 2019; Published: 29 November 2019



**Abstract:** A flame retardant aluminum 2-carboxyethyl-phenyl-phosphinate (CPA-Al) was synthesized through the salification reaction. The molecular structure of CPA-Al and thermal stability were characterized by solid nuclear magnetic resonance, Fourier transform infrared spectroscopy, and thermogravimetric analysis. Subsequently, CPA-Al mixed in polyurethane was coated on polyester textile to obtain flame-retardant samples. The addition of 14.7 wt.% CPA-Al in textile sample can bring a limited oxygen index (LOI) value of 24.5%, 0 s after flame time, and the vertical burning B1 rating. Meanwhile, the incorporated CPA-Al reduced the peak heat release rate, total heat release, average effective heat of combustion, and increased the charring capacity of polyester textiles in contrast to the samples without CPA-Al. CPA-Al exerted not only its flame inhibition effect in gas phase, but also the charring and barrier effect in the condensed phase. Besides, with an increasing CPA-Al ratio in polyester textile, the contact angle gradually decreased from 123.6° to 75.6°, indicating that the surficial property of coating from hydrophobic to hydrophilic, thereby increasing the moisture permeability of polyester textile.

**Keywords:** polyester textile; flame retardant; coating; phosphinate

## 1. Introduction

In the past several decades, polyester textile has been widely applied to garment, upholstery, and decoration, etc. [1,2], because of its excellent properties, such as low cost, being resistant to chemicals, dimensional stability, and good physical features [3–8]. However, polyester textile is flammable and it will melt dripping during combustion, which caused potential fire risks to people's lives and property [9,10]. Therefore, it is necessary to impose flame retardancy to textile in work clothes and tents applications [11,12].

In recent years, some researchers have been trying several kinds of flame retardants, such as brominated flame retardants [13], phosphorus-containing flame retardant [14,15], intumescent flame retardant [16,17], and nanometer flame retardant [18–20] to improve the flame retardancy of polyester textile. Some researchers have been trying to combine some known efficient phosphorus-based characteristic structures or functional groups, such as phosphonate and phosphinate [21–24], cyclotriphosphazene [25–28], and phosphinate-POSS [29,30] to prepare the flame-retardant polyester textile.

There are three ways to acquire flame retardancy to polyester textile [31]: copolymerizing flame-retardant monomer in polyester [32]; incorporating flame-retardant additive into polyester during processing [33]; and treating polyester textile in flame-retardant solution [34]. Treating polyester textile is a feasible method for obtaining flame-retardant textile due to its easy processing way. The treating methods include photo-induced grafting reactions [35], oxygen plasma treatment [36], layer-by-layer (LbL) assembly [37–39], dyeing-like process [40], or sol-gel process [3]; traditional coatings by means of spray-, brush-, or roller techniques [41] and so on. More importantly, a simple and efficient treatment method can reduce the production cost and greatly save manual labour and material resources.

In this thesis, a kind of phosphinate, which was named aluminum 2-carboxyethyl-phenyl-phosphinate (CPA-Al), was successfully synthesized and characterized. Afterwards, CPA-Al incorporated into polyurethane (PU) as back coating materials to prepare flame-retardant polyester textile, which was a simple and convenient way. The flame-retardant properties, mechanism, and surficial property of CPA-Al on polyester textile were investigated.

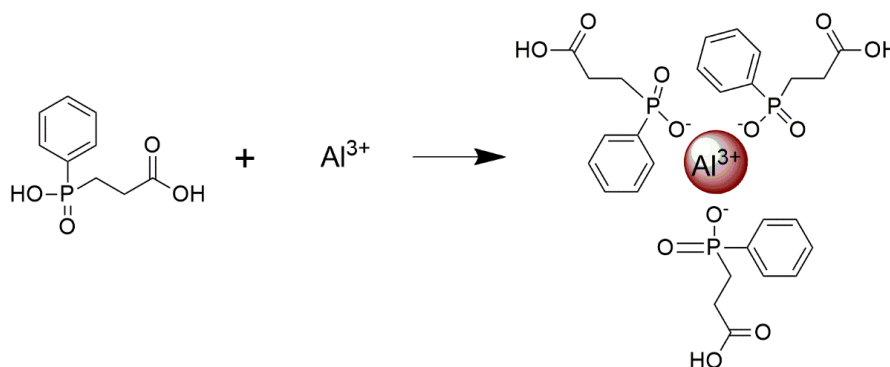
## 2. Experimental

### 2.1. Materials

3-Hydroxyphenylphosphinyl-propanoic acid (CPA) was provided by Dezhou Changxing Chemical New Materials Research and Development Co., Ltd. (Dezhou, China). Aluminum chloride hexahydrate was purchased from Sinopharm Chemical Reagent Co. Ltd. (Beijing, China). Polyester textile (T, weighting 155 g/m<sup>2</sup>, thickness 0.20 mm) was supplied by Jiangsu Shixing Textile Co., Ltd. (Jiangsu, China). Toluene was supplied by Beijing Chemical Works (Beijing, China). Polyurethane (PU, HKW-3055), which was supplied by Haina Environmental Science and Technology (Shandong, China), was prepared by polyester polyols (2024, prepared by adipic acid, ethylene glycol and 1, 4-butylene glycol) that were reacting with diphenyl methane di-isocyanate (MDI) and mixing *N,N*-dimethylformamide (DMF) (70 wt % in PU).

### 2.2. Synthesis of CPA-Al

CPA (128.4 g, 0.6 mol) and 400 mL water were fed into a 1000 mL three-neck flask with a mechanical stirrer. The mixture was stirred and heated to 70 °C in water bath until the CPA completely dissolved in deionized water. Subsequently, the reaction temperature was increased to 90 °C and then stabilized for 30 min. A solution of aluminum chloride hexahydrate (96.6 g, 0.4 mol) in 200 mL water was dripped into the mixture within 30 min. While the solution of aluminum chloride hexahydrate was added into the reaction system, the mixture turned to white emulsion and the reaction was carried out for another 3 h. The reaction mixture was filtered to obtain the solid product and the product was then washed and filtered with water at 80 °C until the PH value of the filtrate remained stable. Finally, the product was dried in a vacuum oven at 120 °C for 3 h. Scheme 1 shows the reaction formula. The yield of CPA-Al was up to 90%.



**Scheme 1.** Synthesis route of 2-carboxyethyl-phenyl-phosphinate (CPA-Al).

### 2.3. Preparation of Flame-Retardant Textiles and the Control Samples

PU, toluene, and CPA-Al were stirred and completely blended at room temperature in a beaker to prepare PU coating. Table 1 lists the formulas of PU, toluene, and CPA-Al in each sample.

**Table 1.** Formulas of the different textile samples.

Samples	Polyester Textile (g)	PU (g)	CPA-Al	
			g	wt %
PU/T	139	18	0	0
7.1%CPA-Al/PU/T	139	18	12	7.1
10.3%CPA-Al/PU/T	139	18	18	10.3
14.7%CPA-Al/PU/T	139	18	27	14.7

The polyester textile was pulled and fixed on the holder and PU coating was then carried out on the back of textiles under about 60 N pressure. The coated textiles were then placed in a drying oven at 160 °C for 3 min. The flame-retardant textiles were labeled as 7.1%CPA-Al/PU/T, 10.3%CPA-Al/PU/T, and 14.7%CPA-Al/PU/T based on the mass ratio of CPA-Al in each sample. The control sample PU/T was also prepared in the same manner, but without the addition of the flame retardant CPA-Al. Table 1 lists the mass fraction of CPA-Al in each textile sample.

### 2.4. Characterization

FTIR spectra were obtained while using a Nicolet iN10MX-type spectrometer (Thermo Nicolet Corp., Madison, WI, USA) over the frequency range of 500 to 4000  $\text{cm}^{-1}$ . Thirty-two scans and eight  $\text{cm}^{-1}$  spectral resolutions were used for each measurement. The powdered samples were thoroughly mixed with KBr and then pressed into pellets.

The  $^1\text{H}$  nuclear magnetic resonance ( $^1\text{H}$  NMR),  $^{13}\text{C}$  NMR,  $^{27}\text{Al}$  NMR, and  $^{31}\text{P}$  NMR data were obtained while using a Bruker 400 MHz WB Solid-State NMR Spectrometer (Karlsruhe, Germany).

Thermogravimetric analysis (TGA) was performed using a PerkinElmer STA 8000 thermal gravimetric analyzer (Perkin Elmer, Waltham, MA, USA). The sample was placed in a platinum crucible and then heated from 50 to 700 °C at the rate of 20 °C/min. in  $\text{N}_2$  atmosphere. All of the tests were repeated three times, and the typical TGA data were reproducible within  $\pm 5\%$ .

The limited oxygen index (LOI) value was measured while using an FTT (Fire Testing Technology, London, UK) Dynisco LOI instrument according to ASTM D2863-97 (sample dimension: 140.0 mm  $\times$  52.0 mm). The LOI measurement for each specimen was repeated three times, and the error values were  $\pm 0.3\%$ . The vertical burning test (Fire Testing Technology, London, UK) was performed while using an FTT0082 instrument according to GB/T 5455 (sample dimension: 300.0 mm  $\times$  80.0 mm). The cone calorimeter test (Fire Testing Technology, London, UK) was performed while using an FTT0007 cone calorimeter according to ISO5660 at an external heat flux of 50  $\text{kW/m}^2$  (sample dimension: 100.0 mm  $\times$  100.0 mm). The measurement for each specimen was repeated twice, and the error values of the typical cone calorimeter data were reproducible within  $\pm 5\%$ .

A STA 8000 TGA thermogravimetric analyzer (Perkin Elmer, Waltham, MA, USA) was coupled to Frontier infrared spectrometer (Perkin Elmer, Waltham, MA, USA) (TGA-FTIR) to detect volatile pyrolysis products. Each sample was placed in an alumina crucible and then heated from 50 to 700 °C at a heating rate of 20 °C/min. under  $\text{N}_2$  atmosphere. The thermogravimetric analyzer and FTIR spectrometer were connected by pipeline at 280 °C.

The SEM images of the residues after cone calorimeter test were obtained while using a Phenom Pro Desktop scanning electron microscope (Phenom World, Eindhoven, Netherlands) at high vacuum conditions with a voltage of 5 kV. The tested specimens were taken from the outer layer of carbon residues after the cone calorimeter test.

The element contents of residues from cone calorimeter were investigated via a PerkinElmer PHI 5300 ESCA X-ray photoelectron spectrometer (XPS, Waltham, MA, USA). The tested specimens were

obtained from the surface of residues with sufficiently mixed and grinded residues, and the results were the average of the three times repeated tests, which were all reproducible within  $\pm 5\%$ .

The contact angles of different polyesters were measured with a Dataphysics OCA-35 contact angle analyzer (DataPhysics Instruments GmbH, Filderstadt, Germany) at room temperature at an ambient atmosphere.

The water vapor permeability of polyesters samples was tested with a relative humidity (RH) of 90% and at the temperature of 23 °C, according to Standard GB/T 1037-1988 (circular samples dimension: 100.0 mm diameter, 0.2 mm thickness). The results were the average of the three times repeated tests.

### 3. Results and Discussion

#### 3.1. Characterization of the Structure and Thermal Stability of CPA-Al

$^1\text{H}$  solid-state NMR,  $^{13}\text{C}$  solid-state NMR,  $^{31}\text{P}$  solid-state NMR, and  $^{27}\text{Al}$  solid-state NMR confirm the structure of CPA-Al, as in Figure 1. In Figure 1a, the chemical shift at 2.49 ppm was attributed to H atoms in ethyl group. H atoms in the benzene ring caused the chemical shift at 5.98, 6.97, and 8.35 ppm. The H atoms in carboxyl should cause the chemical shift between 10–12 ppm. In Figure 1b, the chemical shift at 28.76 and 32.08 ppm was assigned to C atoms in  $-\text{CH}_2-\text{CH}_2$  group. The chemical shift between 128.71–135.00 ppm was caused by C atoms in the benzene ring. The chemical shift at 176.81–180.52 ppm was attributed to C atoms in carboxyethyl group. There was not only one chemical shift between 176.81–180.52 ppm, so the reaction might be generated some by-products. The chemical shift at 23.31 ppm in  $^{31}\text{P}$  NMR was caused by the C–P–C. Combining the results of  $^1\text{H}$  NMR,  $^{13}\text{C}$  NMR, and  $^{31}\text{P}$  NMR, a little of  $-\text{COOH}$  should react with  $\text{Al}^{3+}$ , and Figure 2 shows the structure of the by-product. Therefore, the shift at 36.27–37.94 was caused by the C–P–C bond, which was affected by the  $-\text{COO}-$  of by-product. In Figure 1d, the strong peak at  $-15.65$  ppm was assigned to aluminum atoms in hypophosphite. The aluminum atoms from aluminum carboxylate structure in by-product caused the weak peak at  $-3.04$  ppm. The integral area of the two peaks shows that the ratio of Al in by-product is very rare.

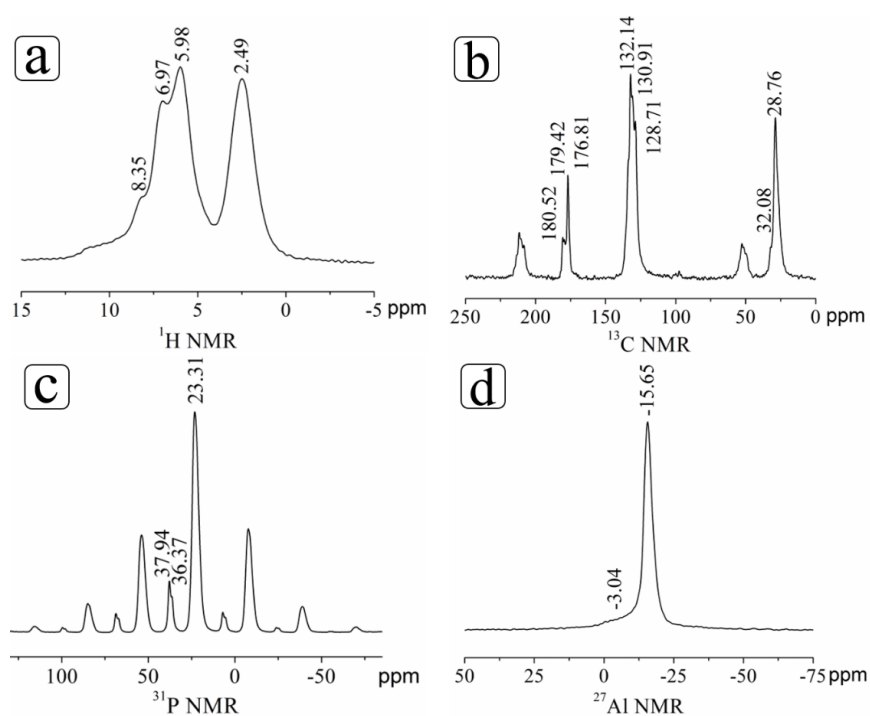


**Figure 1.** Solid-state NMR spectra of CPA-Al. (a)  $^1\text{H}$  NMR; (b)  $^{13}\text{C}$  NMR; (c)  $^{31}\text{P}$  NMR; and (d)  $^{27}\text{Al}$  NMR of CPA-Al.



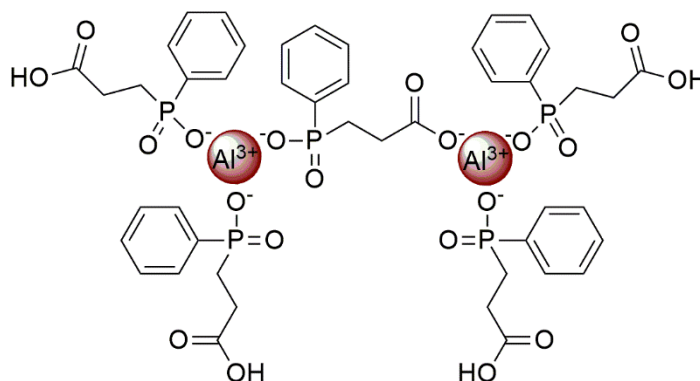


**Figure 2.** The chemical structure of CPA-Al main by-product.

Figure 3 shows the FTTR spectra of reactant CPA and product CPA-Al. The spectra exhibit that the absorption band at  $900\text{ cm}^{-1}$  in CPA spectrum disappeared in CPA-Al. The absorption band at  $900\text{ cm}^{-1}$  represents the deformation vibration of out of plane O–H. The disappearance of this band implies that O–H bond transformed to  $\text{O}^{-}\text{Al}^{3+}$  structure. Absorption at  $1721\text{ cm}^{-1}$  (C=O) has no obvious change in both CPA and CPA-Al, indicating that  $-\text{COOH}$  hardly did attend the salification reaction. Combining with previous discussion in solid-state NMR, it can be deduced that only a little  $-\text{COOH}$  group participated in the salification reaction and little by-products were formed. CPA-Al was successfully synthesized, according to the results.

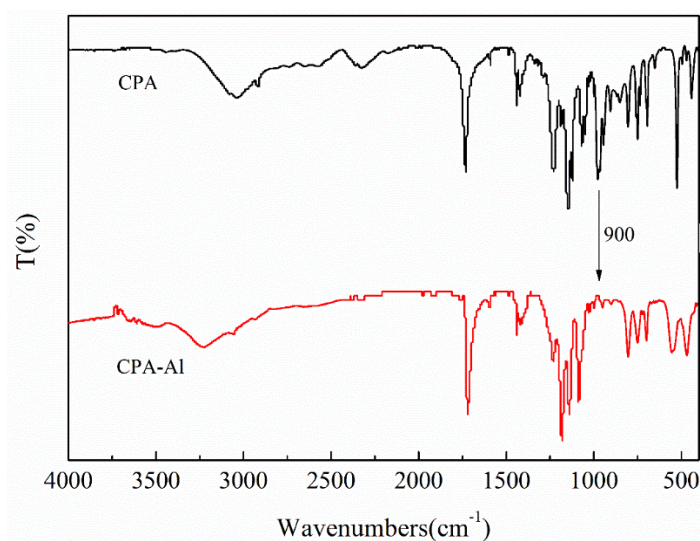


**Figure 3.** FTTR spectra of CPA-Al and 3-Hydroxyphenylphosphinyl-propanoic acid (CPA).

The thermal stability of CPA-Al was also tested by TGA, and Figure 4 and Table 2 show the results. The thermal stability of CPA-Al was outstandingly enhanced when compared with raw material CPA. The onset degradation temperature ( $T_{d, 1\%}$ ) of CPA-Al reached up to  $300\text{ }^{\circ}\text{C}$ . CPA at  $600\text{ }^{\circ}\text{C}$  decomposed completely and no residue nearly was reserved. However, the residue yield of CPA-Al at  $600\text{ }^{\circ}\text{C}$  was 40.1%. All of these results confirm that CPA-Al possessed higher thermal stability and better charring ability, which contributes to bringing better barrier effect to materials.

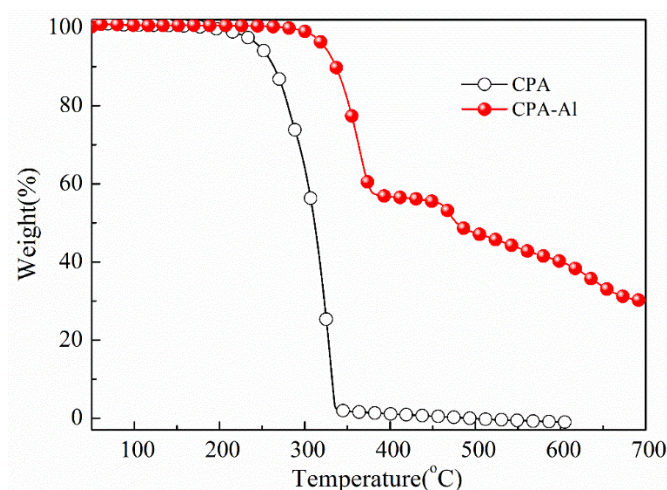


Figure 4. TGA curves of CPA-Al and CPA.

Table 2. Thermogravimetric analysis (TGA) parameters of CPA-Al and CPA.

Samples	T <sub>d,1%</sub> (°C)	T <sub>d,5%</sub> (°C)	Residuals at 600 °C (wt %)	Residuals at 700 °C (wt %)
CPA	214	248	0	–
CPA-Al	300	324	40.1	30.1

### 3.2. LOI and Vertical Burning Test.

CPA-Al was applied in PU coating of polyester textile to investigate its flame retardancy. The flame-retardant properties of the polyester textiles were evaluated while using LOI and vertical burning tests. Table 3 presents the corresponding results. The LOI values of PU/T were only 20.0%. After the CPA-Al was incorporated into the polyester coating, the LOI values of samples gradually increased. The LOI value increased to 24.5% when the mass fraction of CPA-Al in sample was 14.7 wt. %.

Table 3. Limited oxygen index (LOI) value and vertical burning test of textile samples.

Samples	LOI (%)	Vertical Burning Test			
		After Flame Time (s)	The Length of Combustion/cm	Dripping	Rating
PU/T	20.0	32.5	30.0	Yes	NR
7.1%CPA-Al/PU/T	23.6	30.0	16.2	Yes	NR
10.3%CPA-Al/PU/T	23.8	8.8	9.8	Yes	B2
14.7%CPA-Al/PU/T	24.5	0	7.4	No	B1

The after flame time after 12 s exposure time under fire of vertical burning test for PU/T was 32.5 s until the textiles were totally burned out. After flame-retardant CPA-Al was incorporated into the PU, the after flame time shortened obviously when compared with PU/T. It is also clearly observed that the burning distances decreased with increasing mass fraction of CPA-Al in PU coatings. When the mass fraction of CPA-Al in samples reached 14.7% (14.7%CPA-Al/PU/T), it had not any dripping observed and the rating reached to B1 with the 0 s after flame time during the vertical burning test, which disclosed the anti-dripping effect of CPA-Al on polyester textiles during combustion.

Figure 5 was the digital photos of 14.7%CPA-Al/PU/T at different points during the combustion of vertical burning test. The polyester textiles were not ignited by fire and the damage length of the 14.7%CPA-Al/PU/T was caused by the heat of flame and not by combustion. The edge of damaged polyester textile was curly after firing. There was no obvious charring behavior around the damage

edge of 14.7%CPA-Al/PU/T in Figure 5d. All of the phenomena disclose that CPA-Al should effectively inhibit the free radical chain reaction in the gaseous phase during combustion.

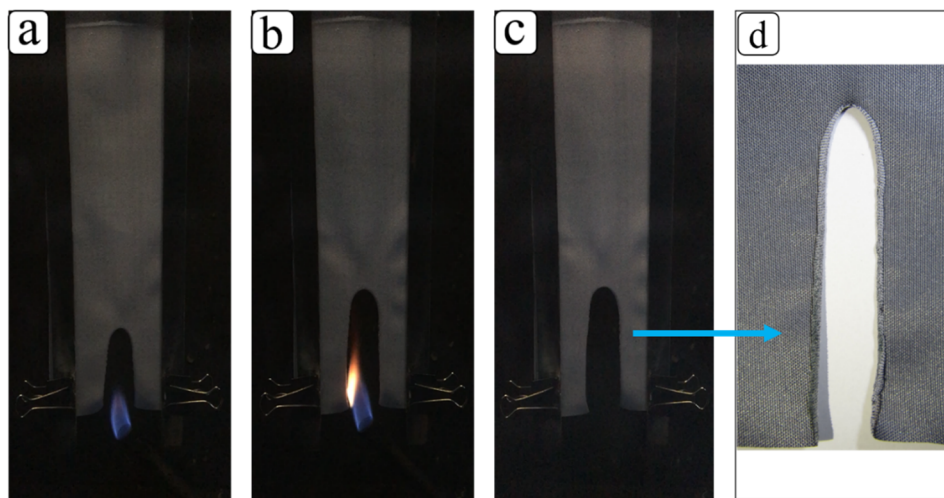


**Figure 5.** Digital photos of 14.7%CPA-Al/PU/T during combustion of vertical burning test. (a) 5 s; (b) 10 s; (c) 15 s; and (d) Partial digital photo.

### 3.3. Cone Calorimeter Test

The cone calorimeter test was conducted to sufficiently investigate the flame-retardant behaviors of CPA-Al in the polyester. Figures 6 and 7 respectively show the curves of heat release rate (HRR) and the curves of mass loss rate (MLR), and Table 4 summarizes the partial typical characteristic parameters, such as peak of heat release rate (PHRR), total smoke release (TSR), average of effective heat of combustion (av-EHC), total heat release (THR), average CO yield (av-COY), average CO<sub>2</sub> yield (av-CO<sub>2</sub>Y), and residue. These data of flame-retardant samples mentioned above were calculated from time 30 s to time 165 s and the dates of PU/T were calculated from 35 to 125 s, according to the curves of heat release rate.

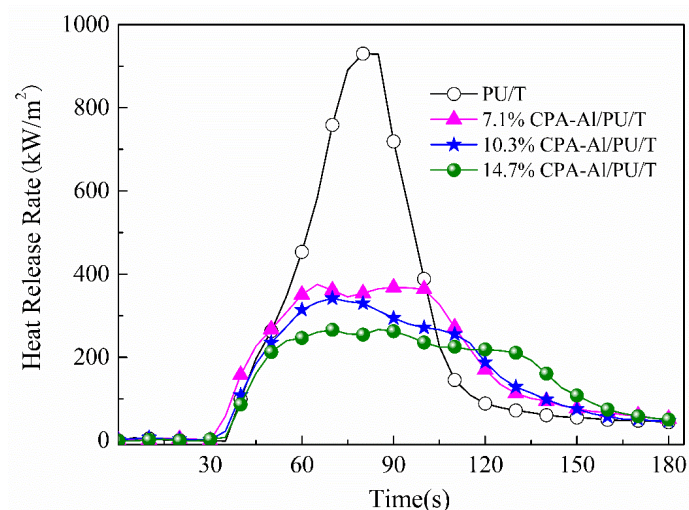


**Figure 6.** Heat release rate (HRR) curves of CPA-Al polyester textiles.

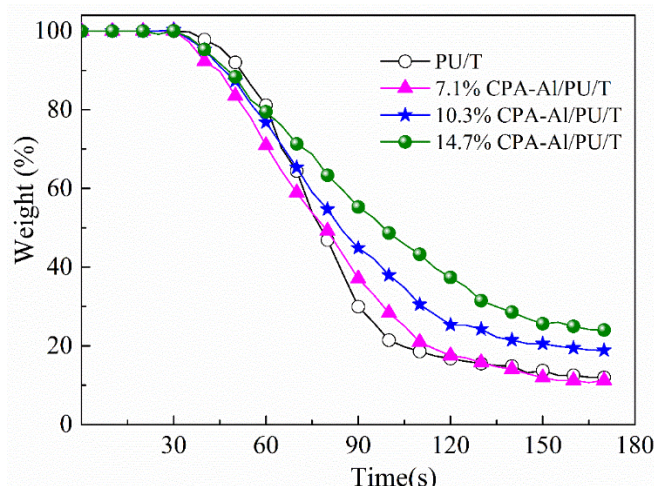


Figure 7. Mass loss rate (MLR) curves of CPA-Al polyester textiles.

Table 4. Cone calorimeter data of CPA-Al polyester samples.

Samples	PHRR (kW/m <sup>2</sup> )	av-EHC (MJ/m <sup>2</sup> )	THR (MJ/m <sup>2</sup> )	TSR (m <sup>2</sup> /m <sup>2</sup> )	av-COY (kg/kg)	av-CO <sub>2</sub> Y (kg/kg)	Residue (wt %)
7.1%CPA-Al/PU/T	375	22.6	29.8	1323	0.11	2.48	11.2
10.3%CPA-Al/PU/T	342	19.4	26.6	1395	0.15	2.69	18.9
14.7%CPA-Al/PU/T	267	16.8	25.2	1438	0.14	2.20	24.0
PU/T	930	25.5	38.2	989	0.07	2.80	11.9

As shown in Table 4 and Figure 6, the PHRR values of CPA-Al/PU/T were distinctly reduced and burning intensity was effectively inhibited. The PHRR of 14.7%CPA-Al/PU/T fell by 71.3% when compared with that of PU/T. There was a sharp peak from the start to the end in the HRR curves of PU/T but the HRR curve of CPA-Al/PU/T was gentle, indicating that CPA-Al exerted better charring and barrier effect. In Table 4, all of the av-EHC values of CPA-Al/PU/T were lower than that of PU/T, and they all gradually decreased with an increasing mass ratio of CPA-Al in samples. EHC can be used to measure burning ratio of combustible volatile gas. The reduction of the av-EHC values indicated that the incorporation of CPA-Al could effectively inhibit the combustion of volatile gas and terminate the free radical chain reaction in gaseous phase.

According to Figure 7 and Table 4, with an increasing ratio of CPA-Al in textiles, the total mass loss (TML) values at the end of combustion obviously increase and more residues were produced, which implies that CPA-Al had an excellent charring effect. The formation of more residues not only enhanced the barrier effect to fire, but also decreased the release of fuels. Due to the incorporation of CPA-Al, the decrease of fuels testified by TML and the incomplete combustion of the flammable gas determined by av-EHC values all contributed to the lower burning intensity and total heat release. The decrease of fuels testified by TML and the incomplete combustion of the flammable gas determined by av-EHC values all contributed to lower burning intensity and total heat release due to incorporation of CPA-Al. In Table 4, the THR values gradually decreased with an increasing fraction of CPA-Al in PU coating, which corresponded to the results discussed.

Similarly, the incomplete combustion in the gaseous phase also led to the more smoke and the more av-COY, which the results in Table 4 proved. The incomplete contents in the gaseous phase would result in the more solid char particles, and accordingly the smoke density of flame-retardant samples would increase. According to Table 4, the flame-retardant samples with CPA-Al produced more CO, less CO<sub>2</sub>, and the higher TSR values. The addition of CPA-Al in samples obviously inhibited the combustion of volatile gas and exerted flame-retardant action in gaseous phase.



### 3.4. TGA and TGA-FTIR Analysis

TGA analysis also further testifies the results in cone calorimeter. Figure 8 shows the TGA curves of polyesters, and Table 5 lists some typical dates. The residual yields at 600 °C of PU/T is only 9.2 wt %, whereas that of CPA-Al/PU/T at 600 °C is from 17.2% to 19.0% with increasing mass fraction of CPA-Al. Therefore, the result further showed the promotion action of CPA-Al on the charring yields of the matrix.

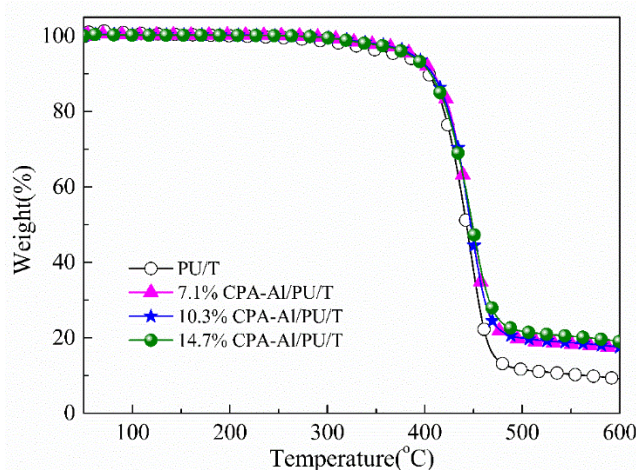
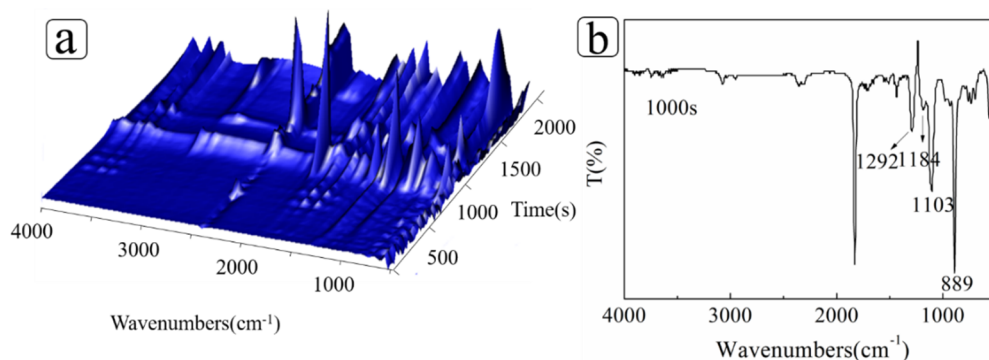


Figure 8. TGA curves of polyester textiles.

Table 5. TGA parameters of polyester textiles.

Samples	T <sub>d, 1%</sub> (°C)	T <sub>d, 5%</sub> (°C)	Residuals at 600 °C (wt %)
PU/T	286	375	9.2
7.1%CPA-Al/PU/T	315	388	17.2
10.3%CPA-Al/PU/T	321	388	17.5
14.7%CPA-Al/PU/T	317	384	19.0

Figure 9 shows the three-dimensional (3D) FTIR spectrum of the pyrolysis gas products of CPA-Al from TGA in order to explore the flame retardant mechanism of CPA-Al in gas phase. The release rate of the decomposed rapidly increased to a maximum value at 1000 s and decreased until around 1300 s, where it had another larger value. In Figure 9a, the gas release trend was in keeping with the TGA results of CPA-Al. Figure 9b shows the FTIR spectra of pyrolysis gas products of CPA-Al at the maximum gas release rate. In this spectrum, the peaks at 1184 and 1103 cm<sup>-1</sup> are attributed to PO<sub>2</sub><sup>-</sup> anion absorption and the peaks at 1292 and 889 cm<sup>-1</sup> can be assigned to P=O and P-O bonds, respectively. The phosphorus-containing groups can quench radicals and reveal the flame-retardant effect in gas phase. The presence of PO<sub>2</sub> and PO in the spectrum provides the basis for CPA-Al in gas phase of flame inhibition effect.



**Figure 9.** (a) Three-dimensional (3D) FTIR spectrum of the pyrolysis gas products of CPA-Al from TGA; (b) FTIR spectra of pyrolysis gas products of CPA-Al at the maximum gas release rate.

### 3.5. The Residue Analysis from Cone Calorimeter Test

Figure 10 shows the digital photos of the residues from cone calorimeter test. As shown in Figure 10a, the PU/T was almost completely combusted and only a few residues of PU/T were left. After CPA-Al was incorporated into PU/T, as shown in Figure 10b, the residue yields and quality of 14.7%CPA-Al/PU/T obviously increased. CPA-Al promoted the charring process of polyester textiles during combustion and exerted a barrier effect of the char layer in condensed phase.

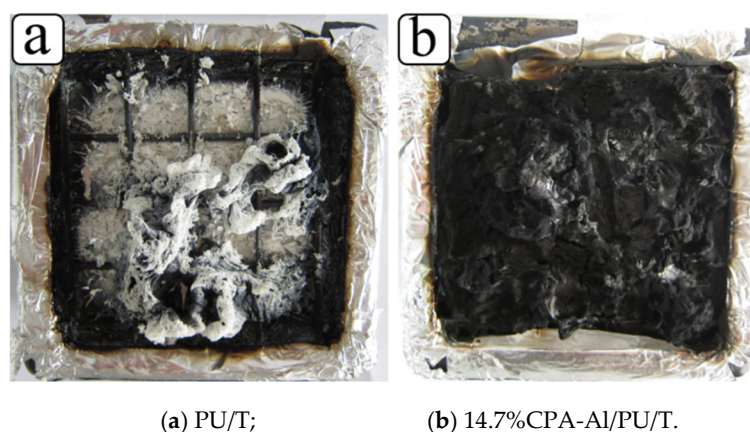


**Figure 10.** Digital photos of polyester residues from cone calorimeter.

SEM analysis of 14.7%CPA-Al/PU/T was conducted in order to explore the microscopic morphology of residue further, and the results are shown in Figure 11. There were many bosomy and sealed bubble-shaped structures with different sizes in Figure 11a. In Figure 11b, the bubble-shaped structure was clearly observed and the structure is continuous and sealed with many wrinkles. The residue structure of 14.7%CPA-Al/PU/T can inhibit the exchange of the fuel and oxygen and efficiently protect the polyester from the flame. The continuous and sealed char layer of 14.7%CPA-Al/PU/T blocked the volatile gas generated by polyester, and then cut off the fuel supply, and ultimately weakened the combustion intensity. The results confirm that the incorporation of CPA-Al should promote the formation of sealed and flexible char layer. The results also further support the flame-retardant effect of CPA-Al in the condensed phase.



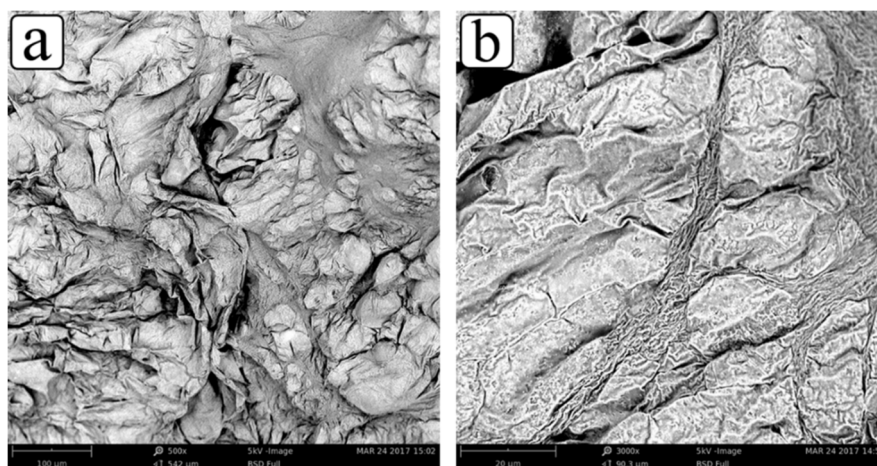


**Figure 11.** SEM photos of 14.7%CPA-Al/PU/T residue from cone calorimeter. (a) 500×; (b) 3000×.

The element contents of PU/T and CPA-Al/PU/T residues from the cone calorimeter tests were determined via XPS. Table 6 lists the results. The phosphorus content in residues has an obvious up tendency with increasing the mass ratio of CPA-Al in samples, indicating that more phosphorus contents joined the charring process and promoted the formation of phosphorus-rich residue, thereby bringing a better barrier effect on heat and fire.

**Table 6.** Element contents of residues from the cone calorimeter test.

Samples	Element Content (wt %)				
	C	N	O	Al	P
7.1%CPA-Al/PU/T	77.64	2.07	15.98	1.74	2.57
10.3%CPA-Al/PU/T	70.67	1.88	19.17	3.36	4.92
14.7%CPA-Al/PU/T	69.55	3.01	19.34	2.81	5.29
PU/T	75.84	2.98	21.18	–	–

### 3.6. Barrier Performance of CPA-Al/PU/T

Table 7 shows the results of water vapor permeation. The amounts water vapor permeation of CPA-Al/PU/T samples all highly increased when compared with PU/T and the water vapor permeation of 14.7%CPA-Al/PU/T was up to 1648.6 g/m<sup>2</sup>·day. The addition of CPA-Al improved the moisture permeability of polyester textiles. The contact angle test was carried out to probe the reason for the change of water vapor permeation, and the results are shown in Table 7 and Figure 12. With an increasing CPA-Al ratio in polyester textile, the contact angle gradually decreased from 123.6° to 75.6°. Due to the carboxyl functional group of CPA-Al being a hydrophilic group, the contact angle of polyester textile will be reduced, indicating that the polyester textile changed their surficial property from hydrophobic to hydrophilic [42–44]. That is why the amounts of water vapor permeation gradually increased [45].

**Table 7.** Water vapor permeation and contact angles of CPA-Al/PU/T.

Samples	Water Vapor Permeation (g/m <sup>2</sup> ·day)	Contact Angle (°)
PU/T	690.3	123.6
7.1%CPA-Al/PU/T	1091.2	99.8
10.3%CPA-Al/PU/T	1280.4	92.5
14.7%CPA-Al/PU/T	1648.6	75.6

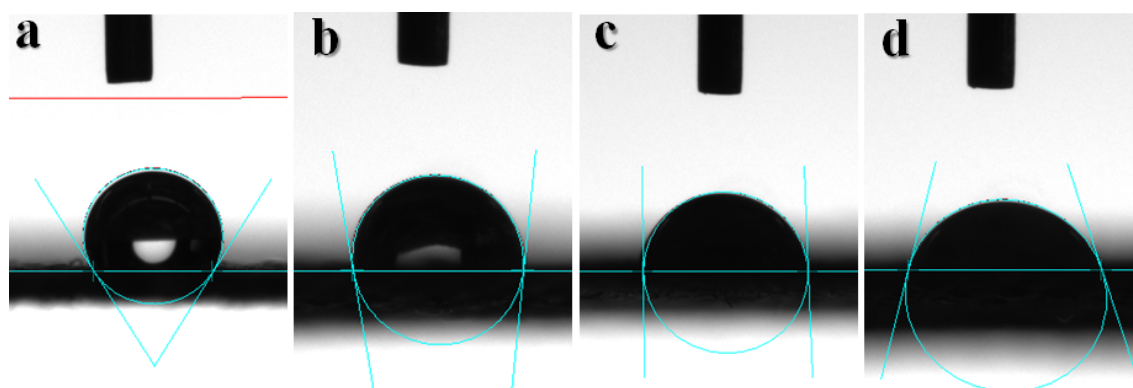


**Figure 12.** Digital images of the contact angle experiment. (a) PU/T; (b) 7.1%CPA-Al/PU/T; (c) 10.3%CPA-Al/PU/T; and, (d) 14.7%CPA-Al/PU/T.

#### 4. Conclusions

A flame-retardant additive CPA-Al was successfully synthesized and characterized. The polyester textile with 14.7 wt.% CPA-Al obtained a LOI value of 24.5%, after a flame time of 0 s, self-extinguishment, shorter burning distance, and B1 rating in the vertical flame test. The incorporated CPA-Al also decreased the PHRR, av-EHC, THR, and increased the charring capacity of polyester textile. The flame-retardant effect of CPA-Al resulted from not only flame inhibition effect in gaseous phase, but also the charring and barrier effect of flexible and sealed char layer in the condensed phase. Therefore, CPA-Al in the PU coating can endow polyester textile with better flame-retardant effect. Besides, with an increasing CPA-Al ratio in polyester textile, the contact angle gradually decreased from  $123.6^\circ$  to  $75.6^\circ$ . The result revealed that CPA-Al could increase the moisture permeability of polyester textile by means of changing the surficial property of coating from hydrophobic to hydrophilic [46].

**Author Contributions:** Data curation, Z.Y. and X.L.; Investigation, Z.Y.; Methodology, X.L.; Supervision, L.Q.; Writing—original draft, Z.Y.; Writing—review & editing, Y.C., B.X. and Y.Q.

**Funding:** This work was supported by National Natural Science Foundation of China (No. 51973006), Project of Great Wall Scholar from Beijing Municipal Commission of Education (CIT&TCD20180312), Beijing Talents Project (No. 2018A39).

**Conflicts of Interest:** The authors declare no conflict of interest.

#### References

- Li, S.N.; Huang, S.; Xu, F.; Xiao, H.; Zhang, F.X.; Zhang, G.X. Preparing polyester/carbon multifunctional fabrics by phosphoric acid carbonization. *Cellulose* **2019**, *26*, 8907–8917. [[CrossRef](#)]
- Alongi, J.; Carosio, F.; Kiekens, P. Recent Advances in the Design of Water Based-Flame Retardant Coatings for Polyester and Polyester-Cotton Blends. *Polymers* **2016**, *8*, 357. [[CrossRef](#)] [[PubMed](#)]
- Guido, E.; Alongi, J.; Colleoni, C.; Blaio, A.D.; Carosio, F.; Verelst, M.; Malucelli, G.; Rosace, G. Thermal stability and flame retardancy of polyester fabrics sol-gel treated in the presence of boehmite nanoparticles. *Polym. Degrad. Stab.* **2013**, *98*, 1609–1616. [[CrossRef](#)]
- Didane, N.; Giraud, S.; Devaux, E. Fire performances comparison of back coating and melt spinning approaches for PET covering textiles. *Polym. Degrad. Stab.* **2012**, *97*, 1083–1089. [[CrossRef](#)]
- Miyake, Y.; Tokumura, M.; Nakayama, H.; Wang, Q.; Amagai, T.; Ogo, S.; Kume, K.; Kobayashi, T.; Takasu, S.; Ogawa, K.; et al. Simultaneous determination of brominated and phosphate flame retardants in flame-retarded polyester curtains by a novel extraction method. *Sci. Total Environ.* **2017**, *601*, 1333–1339. [[CrossRef](#)] [[PubMed](#)]
- Wrobel, G.; Liu, C.H.; Piech, M.; Dardona, S.; Gao, P.X. Synthesis and Thermal Degradation of Fire-Retardant Zinc Hydroxystannate Nanocube Coated Textiles. *Sci. Adv. Mater.* **2012**, *4*, 819–824. [[CrossRef](#)]
- Behera, K.; Chang, Y.H.; Chiu, F.C.; Yang, J.C. Characterization of poly (lactic acid) s with reduced molecular weight fabricated through an autoclave process. *Polym. Test.* **2017**, *60*, 132–139. [[CrossRef](#)]

8. Behera, K.; Sivanjineyulu, V.; Chang, Y.H.; Chiu, F.C. Thermal properties, phase morphology and stability of biodegradable PLA/PBSL/HAp composites. *Polym. Degrad. Stab.* **2018**, *154*, 248–260. [[CrossRef](#)]
9. Feng, Q.L.; Gu, X.Y.; Zhang, S.; Zhao, B.; Sun, J.; Li, X.Y.; Dong, M.Z. An Antidripping Flame Retardant Finishing for Polyethylene Terephthalate Fabric. *Ind. Eng. Chem. Res.* **2012**, *51*, 14708–14713. [[CrossRef](#)]
10. Mayer-Gall, T.; Plohl, D.; Derksen, L.; Lauer, D.; Neldner, P.; Ali, W.; Fuchs, S.; Gutmann, J.S.; Opwis, K. A Green Water-Soluble Cyclophosphazene as a Flame Retardant Finish for Textiles. *Molecules* **2019**, *24*, 3100. [[CrossRef](#)]
11. Malucelli, G. Biomacromolecules and Bio-Sourced Products for the Design of Flame Retarded Fabrics: Current State of the Art and Future Perspectives. *Molecules* **2019**, *24*, 3774. [[CrossRef](#)] [[PubMed](#)]
12. Horrocks, A.R. Textile flammability research since 1980—Personal challenges and partial solutions. *Polym. Degrad. Stab.* **2013**, *98*, 2813–2824. [[CrossRef](#)]
13. Feng, H.S.; Qiu, Y.; Qian, L.J.; Chen, Y.J.; Xu, B.; Xin, F. Flame Inhibition and Charring Effect of Aromatic Polyimide and Aluminum Diethylphosphinate in Polyamide 6. *Polymers* **2019**, *11*, 74. [[CrossRef](#)] [[PubMed](#)]
14. Sag, J.; Goedderz, D.; Kukla, P.; Greiner, L.; Schönberger, F.; Döring, M. Phosphorus-Containing Flame Retardants from Biobased Chemicals and Their Application in Polyesters and Epoxy Resins. *Molecules* **2019**, *24*, 3746. [[CrossRef](#)] [[PubMed](#)]
15. Lim, K.S.; Bee, S.T.; Sin, L.T.; Tee, T.T.; Ratnam, C.T.; Hui, D.; Rahmat, A.R. A review of application of ammonium polyphosphate as intumescent flame retardant in thermoplastic composites. *Compos. Part B* **2016**, *84*, 155–174. [[CrossRef](#)]
16. Zhou, Y.; Cui, Y.Z.; Liu, G.J.; Lv, L.H. Reach on P/N Type Intumescent Flame Retardant for Polyester Fabric. *Adv. Mater. Res.* **2013**, *785*, 714–717. [[CrossRef](#)]
17. Wattanananom, W.; Churuchinda, S.; Potiyaraj, P. Intumescent flame retardant finishing of polyester fabrics via the layer-by-layer assembly technique. *Int. J. Cloth. Sci. Technol.* **2017**, *29*, 96–105. [[CrossRef](#)]
18. Zhang, J.J.; Ji, Q.; Shen, X.H.; Xia, Y.Z.; Tan, W.; Wang, F.J.; Kong, Q.S. Flame retardancy and non-isothermal crystallization behaviour of PET/TiO<sub>2</sub> nanocomposites. *Polym. Polym. Compos.* **2012**, *20*, 399–406. [[CrossRef](#)]
19. Zhang, J.J.; Ji, Q.; Zhang, P.; Xia, Y.Z.; Kong, Q.S. Thermal stability and flame-retardancy mechanism of poly (ethylene terephthalate)/boehmite nanocomposites. *Polym. Degrad. Stab.* **2010**, *95*, 1211–1218. [[CrossRef](#)]
20. Carosio, F.; Alongi, J.; Malucelli, G.  $\alpha$ -Zirconium phosphate-based nanoarchitectures on polyester fabrics through layer-by-layer assembly. *J. Mater. Chem.* **2011**, *21*, 10370–10376. [[CrossRef](#)]
21. Si, M.M.; Feng, J.; Hao, J.W.; Xu, L.S.; Du, J.X. Synergistic flame retardant effects and mechanisms of nano-Sb<sub>2</sub>O<sub>3</sub>, in combination with aluminum phosphinate in poly (ethylene terephthalate). *Polym. Degrad. Stab.* **2013**, *100*, 70–78. [[CrossRef](#)]
22. Alongi, J. Investigation on flame retardancy of poly (ethylene terephthalate) for plastics and textiles by combination of an organo-modified sepiolite and Zn phosphinate. *Fibers Polym.* **2011**, *12*, 166–173. [[CrossRef](#)]
23. Yang, W.; Song, L.; Hu, Y.; Lu, H.D.; Yuen, R.K.K. Enhancement of fire retardancy performance of glass-fibre reinforced poly (ethylene terephthalate) composites with the incorporation of aluminum hypophosphite and melamine cyanurate. *Compos. Part B* **2011**, *42*, 1057–1065. [[CrossRef](#)]
24. Sonnier, R.; Otazaghine, B.; Vagner, C.; Bier, F.; Six, J.L.; Durand, A.; Vahabi, H. Exploring the Contribution of Two Phosphorus-Based Groups to Polymer Flammability via Pyrolysis–Combustion Flow Calorimetry. *Materials* **2019**, *12*, 2961. [[CrossRef](#)] [[PubMed](#)]
25. Zhang, X.; Zhang, L.P.; Wu, Q.; Mao, Z.P. The influence of synergistic effects of hexakis (4-nitrophenoxy) cyclotriphosphazene and POE-g-MA on anti-dripping and flame retardancy of PET. *J. Ind. Eng. Chem.* **2013**, *19*, 993–999. [[CrossRef](#)]
26. Li, J.W.; Pan, F.; Xu, H.; Zhang, L.P.; Zhong, Y.; Mao, Z.P. The flame-retardancy and anti-dripping properties of novel poly (ethylene terephthalate)/cyclotriphosphazene/silicone composites. *Polym. Degrad. Stab.* **2014**, *110*, 268–277. [[CrossRef](#)]
27. Li, J.W.; Zeng, X.D.; Kong, D.Z.; Xu, H.; Zhang, L.P.; Zhong, Y.; Sui, X.F.; Mao, Z.P. Synergistic effects of a novel silicon-containing triazine charring agent on the flame-retardant properties of poly (ethylene terephthalate)/hexakis (4-phenoxy) cyclotriphosphazene composites. *Polym. Compos.* **2018**, *39*, 858–868. [[CrossRef](#)]
28. Wang, J.N.; Su, X.Y.; Mao, Z.P. The flame retardancy and thermal property of poly (ethylene terephthalate)/cyclotriphosphazene modified by montmorillonite system. *Polym. Degrad. Stab.* **2014**, *109*, 154–161. [[CrossRef](#)]

29. Didane, N.; Giraud, S.; Devaux, E.; Lemort, G.; Capon, G. Thermal and fire resistance of fibrous materials made by PET containing flame retardant agents. *Polym. Degrad. Stab.* **2012**, *97*, 2545–2551. [[CrossRef](#)]
30. Didane, N.; Giraud, S.; Devaux, E.; Lemort, G. Development of fire resistant PET fibrous structures based on phosphinate-POSS blends. *Polym. Degrad. Stab.* **2012**, *97*, 879–885. [[CrossRef](#)]
31. Tang, H.Y.; Chen, J.Y.; Guo, Y.H. A novel process for preparing anti-dripping polyethylene terephthalate fibers. *Mater. Des.* **2010**, *31*, 3525–3530. [[CrossRef](#)]
32. Yang, S.; Kim, J.P. Flame retardant polyesters. III. Fibers. *J. Appl. Polym. Sci.* **2008**, *108*, 2297–2300. [[CrossRef](#)]
33. Wu, Z.H.; Li, L.L.; Jiang, S.S.; Hu, Z.X.; Mao, Y.C.; Zhu, M.F. Preparation and Properties of Recycled-Polyester Nanocomposite Fibers Synergistic Modified with Phosphorus Containing Flame-Retardant and  $\alpha$ -zirconium Phosphate. *Mater. Sci. Forum* **2014**, *789*, 174–177. [[CrossRef](#)]
34. Li, Q.L.; Huang, F.Q.; Jiang, X.J.; Wen, D.; Feng, X.N.; Wu, K. Preparation and properties of a washable flame-retardant coated fabric. *Indian J. Fibre Text.* **2016**, *41*, 40–46.
35. Yu, L.; Zhang, S.; Liu, W.; Zhu, X.J.; Chen, X.P.; Chen, X.S. Improving the flame retardancy of PET fabric by photo-induced grafting. *Polym. Degrad. Stab.* **2010**, *95*, 1934–1942. [[CrossRef](#)]
36. Ömeroğulları, Z.; Kut, D. Application of low-frequency oxygen plasma treatment to polyester fabric to reduce the amount of flame retardant agent. *Text. Res. J.* **2012**, *82*, 613–621. [[CrossRef](#)]
37. Carosio, F.; Alongi, J.; Malucelli, G. Flammability and combustion properties of ammonium polyphosphate-/poly (acrylic acid)-based Layer by Layer architectures deposited on cotton, polyester and their blends. *Polym. Degrad. Stab.* **2013**, *98*, 1626–1637. [[CrossRef](#)]
38. Carosio, F.; Laufer, G.; Alongi, J.; Camino, G.; Grunlan, J.C. Layer-by-layer assembly of silica-based flame retardant thin film on PET fabric. *Polym. Degrad. Stab.* **2011**, *96*, 745–750. [[CrossRef](#)]
39. Jiang, Z.L.; Wang, C.S.; Fang, S.Y.; Ji, P.; Wang, H.P.; Ji, C.C. Durable flame-retardant and antidroplet finishing of polyester fabrics with flexible polysiloxane and phytic acid through layer-by-layer assembly and sol-gel process. *J. Appl. Polym. Sci.* **2018**, *135*, 1–10. [[CrossRef](#)]
40. Gonçalves, A.G.; Jarrais, B.; Pereira, C.; Morgado, J.; Freire, C.; Pereira, M.F.R. Functionalization of textiles with multi-walled carbon nanotubes by a novel dyeing-like process. *J. Mater. Sci.* **2012**, *47*, 5263–5275. [[CrossRef](#)]
41. Liang, S.Y.; Neisius, N.M.; Gaan, S. Recent developments in flame retardant polymeric coatings. *Prog. Org. Coat.* **2013**, *76*, 1642–1665. [[CrossRef](#)]
42. Liu, C.; Fang, Y.F.; Miao, X.M.; Pei, Y.B.; Yan, Y.; Xiao, W.J.; Wu, L.B. Facile fabrication of superhydrophobic polyurethane sponge towards oil-water separation with exceptional flame-retardant performance. *Sep. Purif. Technol.* **2019**, *229*, 1–10. [[CrossRef](#)]
43. Liu, L.B.; Xu, Y.; Li, S.; Xu, M.J.; He, Y.T.; Shi, Z.X.; Li, B. A novel strategy for simultaneously improving the fire safety, water resistance and compatibility of thermoplastic polyurethane composites through the construction of biomimetic hydrophobic structure of intumescent flame retardant synergistic system. *Compos. B* **2019**, *176*, 1–14.
44. Wu, C.; Wang, X.D.; Zhang, J.Y.; Cheng, J.; Shi, L. Microencapsulation and Surface Functionalization of Ammonium Polyphosphate via In-Situ Polymerization and Thiol-Ene Photogated Reaction for Application in Flame-Retardant Natural Rubber. *Ind. Eng. Chem. Res.* **2019**, *58*, 17346–17358.
45. Hicyilmaz, A.S.; Altin, Y.; Bedeloglu, A. Polyimide-coated fabrics with multifunctional properties: Flame retardant, UV protective, and water proof. *J. Appl. Polym. Sci.* **2019**, *136*, 1–10. [[CrossRef](#)]
46. Yadav, M.; Chiu, F.C. Cellulose nanocrystals reinforced  $\kappa$ -carrageenan based UV resistant transparent bionanocomposite films for sustainable packaging applications. *Carbohydr. Polym.* **2019**, *211*, 181–194. [[CrossRef](#)]

